PHYSICAL REVIEW B VOLUME 59, NUMBER 10 1 MARCH 1999-II

Nonlocal current-field relation and the vortex-state magnetic properties of YNi_2B_2C

K. J. Song
Department of Physics, University of Tennessee, Knoxville, Tennessee 37996-1200

J. R. Thompson
Oak Ridge National Laboratory, Oak Ridge, Tennessee 37831-6061
and Department of Physics, University of Tennessee, Knoxville, Tennessee 37996-1200

M. Yethiraj and D. K. Christen
Oak Ridge National Laboratory, Oak Ridge, Tennessee 37831-6061

C. V. Tomy and D. McK. Paul
Department of Physics, University of Warwick, Coventry CV4 7AL, United Kingdom
(Received 1 October 1998; revised manuscript received 23 October 1998)

The equilibrium magnetization M of single crystal YNi_2B_2C superconductor has been studied with magnetic field $H\|c$ axis. The material is clean, with low electrical resistivity and weak magnetic hysteresis (for $H=10$ kG, the critical current density is less than 10^{-6} of the depairing current density). The magnetization $M(H)$ deviates from conventional London predictions, but is well described by recent nonlocal London theory, with well-behaved superconductive parameters. The temperature dependence of the London penetration depth $\lambda(T)$ and other parameters are deduced. [S0163-1829(99)50810-2]

The nickel-borocarbide superconductors are proving to be a rich and complex system of materials. Despite their relatively simple tetragonal structure, modest transition temperatures T_c (an order of magnitude below the high-temperature superconductors), and absence of superconductive CuO layers, the vortex (mixed) state is providing many surprises. Let us recall that *isotropic* superconductors have a simple hexagonal flux-line lattice (FLL) with vortices forming equilateral triangles having an ''opening angle'' β of 60°. In contrast, neutron-scattering studies have shown that the vortex lattice in borocarbides is more complex, even for YNi_2B_2C that contains no magnetic rare-earth ions. Consider the simplest case in which the magnetic field H is applied parallel to the tetragonal $(00c)$ axis and the local supercurrent density $\mathbf{j}(\mathbf{r})$ of a vortex circulates in the basal plane *ab* having square crystallographic symmetry. Then the FLL is (nearly) hexagonal in low fields H where vortices are far apart; with increasing but still modest field levels, the FLL appears to undergo a first-order structural transition;[1,2] and at still higher fields, the lattice becomes *square* (opening angle $\beta\approx 90°$).[3,4] This seemingly strange behavior has been explained in terms of nonlocal London theory[5] or generalized Ginzburg-Landau theory.[4] The present magnetic study gives strong, independent evidence for pronounced nonlocality effects in clean single crystal YNi_2B_2C.

The behavior of the vortex lattice is quite unusual and difficult to explain within standard theories, even those incorporating an anisotropy of the superconductive effective mass. Historically, conventional London theory has been very useful, in that it is valid at all temperatures. However, with the supercurrent $\mathbf{j}(\mathbf{r})$ flowing in the *ab* plane with square symmetry, the London model yields an isotropic vortex-vortex interaction. Hence standard London theory cannot account for either the symmetry of the FLL in YNi_2B_2C or for features in the equilibrium magnetization that are discussed below. This theory is local, in that it assumes a direct proportionality between the vector potential $\mathbf{a}(\mathbf{r})$ and $\mathbf{j}(\mathbf{r})$. Recently, however, Kogan *et al.*[6] have argued that when the electronic mean free path is long, one should include contributions to $\mathbf{j}$ from nearby fields within a nonlocality radius ρ, which is of the order of the BCS coherence length ξ_0 at $T=0$. In Fourier space, one has $(4\pi/c)j_i(\mathbf{k}) = -(1/\lambda^2)Q_{ij}(\mathbf{k})a_j(\mathbf{k})$ with summation over repeated subscripts; the kernel Q_{ij} depends explicitly on $\mathbf{k}$. The resulting *nonlocal* London theory has provided a good description of FLL's and even predicted the lattice transformation at low fields.[5] To date, however, there has been no independent corroborating evidence for the validity of this approach.

If the superconductivity in ''clean'' YNi_2B_2C is indeed nonlocal, then its equilibrium mixed-state properties should be modified significantly.[6,7] In this work, we show that the equilibrium magnetization of single-crystal YNi_2B_2C deviates significantly from simple London predictions, but it is well described by a nonlocal generalization of London theory. These results give strong, independent support for pronounced effects of nonlocality in this borocarbide superconductor, bolster the underlying London-based theory, and provide revised values for the superconductive length scales in YNi_2B_2C.

Standard local London theory provides a simple logarithmic field dependence for the equilibrium magnetization. For intermediate fields $H_{c1}\ll H\ll H_{c2}$, one has[8]

$$M = -M_0 \ln(\eta H_{c2}/H), \quad M_0 = \phi_0/32\pi^2\lambda_{ab}^2. \qquad (1)$$

Here η is a constant of order unity; λ_{ab} is the London penetration depth corresponding to screening by currents in the *ab* plane, with $H\|c$ axis; $H_{c2}=\phi_0/2\pi\xi^2$ is the upper critical

field with ξ being the Ginzburg-Landau coherence length at temperature T. In the Kogan-Gurevich nonlocal formulation of London theory,[6] there is a third independent length scale, the nonlocality radius ρ that depends on the mean free path and temperature. When nonlocality is important, the scale $H_{c2} \sim \phi_0/\xi^2$ for M is replaced by another field scale $H_0 \sim \phi_0/\rho^2$, where the length ρ (unlike ξ) slowly *decreases* with increasing temperature. The resulting expression for M is[6]

$$M = -M_0\left[\ln\left(\frac{H_0}{H}+1\right) - \frac{H_0}{(H_0+H)} + \zeta\right]. \qquad (2)$$

Here $M_0 \propto 1/\lambda^2$ is the same as above, $H_0 = \phi_0/(4\pi^2\rho^2)$ for a square FLL, and $\zeta(T) = \eta_1 - \ln(H_0/\eta_2 H_{c2} + 1)$, where both η_1 and η_2 are constants of order unity. Note that as the temperature increases, H_0 becomes larger while H_{c2} tends toward zero. These differing temperature dependencies mean that for clean materials, the nonlocal form Eq. (2) reduces to the local expression Eq. (1) as T approaches T_c; for dirty materials where ρ is short and H_0 is large, the nonlocal expression collapses to the local form *at all temperatures*–hence the nonlocal formulation contains the standard form as a special case. In summary, the nonlocal theory predicts that the ''clean'' equilibrium magnetization should vary logarithmically with field near T_c, but it progressively and significantly deviates from logarithmic behavior at low temperatures and follows Eq. (2) instead.

The single-crystal sample was grown by a high-temperature flux method using Ni_2B flux with isotopic ^{11}B to reduce neutron absorption. The 17 mg crystal ($0.3\times0.32\times0.05\,cm^3$) had a mosaic spread of less than 0.2°, as determined by neutron diffraction. Magnetic studies were conducted in a superconducting quantum interference device (SQUID) -based magnetometer (Quantum Design MPMS-7), with the crystal glued onto a thin Si disk and mounted in a Mylar tube for measurement. The superconductive transition temperature $T_c = 14.5$ K (measured in $H = 10$ G) was defined as the point at which the linearly varying magnetization $M(T)$ extrapolated to zero. This ignores a very slight ''tail'' with an onset of 15.6 K. In the mixed state, hysteresis loops $M(T)$ were measured in fields up to 6.5 T. The values of magnetization with $H \| c$ have been corrected for the (nearly temperature-independent) normal-state background moment, measured at $T = 20$ K. To obtain the equilibrium (reversible) magnetization in the presence of *slight* hysteresis, we average the increasing- and decreasing-field values. Measurement of the electrical resistivity using a van der Pauw method yielded an electrical resistivity of 4 $\mu\Omega$ cm at 20 K and a residual resistance ratio of 10.

Overall, the magnetic response of this material is remarkably reversible. This is evident in Fig. 1(a), which shows the magnetization at $T = 5$ K with the magnetic field applied parallel to the c axis. At this relatively low temperature $T \approx T_c/3$, there is a wide reversible region; in an earlier study, Ming Xu *et al.*[9] found similar reversibility, meaning that thermodynamics can be used to analyze the material. To illustrate the crystal's reversibility, note that a Bean model analysis of the magnetic hysteresis ΔM at 10 kOe indicates a critical current density $J_c = 100\,A/cm^2$; see Fig. 1(b) for values of J_c at 3, 5, and 7 K. The in-field J_c is small, only

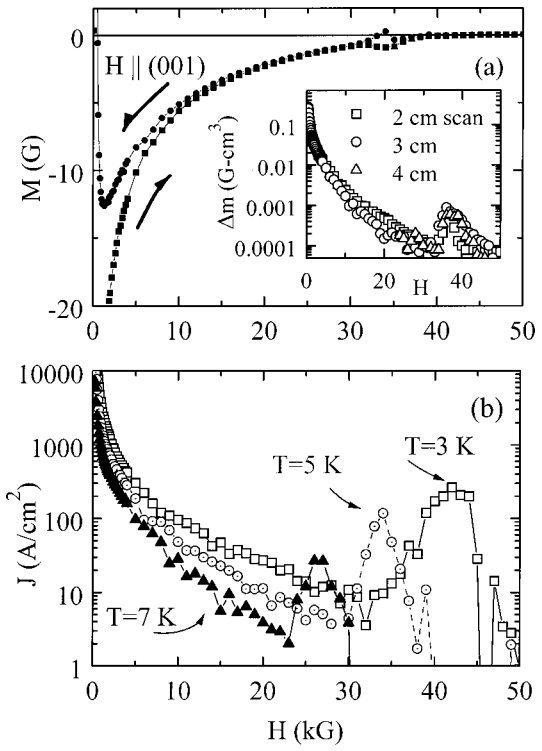

FIG. 1. For YNi_2B_2C single crystal with magnetic field $H \| c$ axis (001). (a) the superconductive magnetization M versus H at 5 K. It is almost completely reversible over a wide range of field and M reduces to zero at 38 kOe. (b) the critical current density obtained using the Bean model. The peak effect observed near H_{c2} arises from weak vortex pinning; see, e.g., Ref. 2. Inset: the irreversible magnetic moment Δm at 4.2 K versus H, for measurement scan lengths of 2, 3, and 4 cm.

$\sim 10^{-6}$ of the depairing current density $J_0 \approx 1.5\times10^8\,A/cm^2$. Since the sample is moved during a measurement scan, we also verified that the scan length has negligible influence on the equilibrium magnetization. The influence of scan length on the *irreversible* magnetic moment m was slight, as illustrated by plots of the irreversible magnetic moment $\Delta m = (m_{decr} - m_{incr})$ at 4.2 K versus H for scan lengths of 2, 3, and 4 cm in the inset to Fig. 1. Normally, scans of 3 cm were used.

Now consider the magnetic field dependence of the magnetization. To visualize the difference between local and nonlocal London behavior, we plot M versus $\ln(H)$ in Fig. 2. In the high-temperature region, the plot is linear (dashed lines), as predicted by Eq. (1). At lower temperatures, however, the data deviate progressively from this simple, ''straight line'' dependence and develop substantial curvature, as is quite evident in the figure. This is just the region where nonlocality effects should become significant. Indeed, the nonlocal expression, Eq. (2), describes the experimental results very well—the solid lines in Fig. 2 show this relation fitted to the data for temperatures $T \leqslant 10$ K. The high quality of these fits supports the premise that nonlocal effects play an important role in ''clean'' borocarbide superconductors.

In addition to a precise description of experimental data, it is essential for comparison with the theory that the resulting parameters—H_0, M_0, and ζ—should behave as the theory prescribes. The three parameters used to fit the data arise

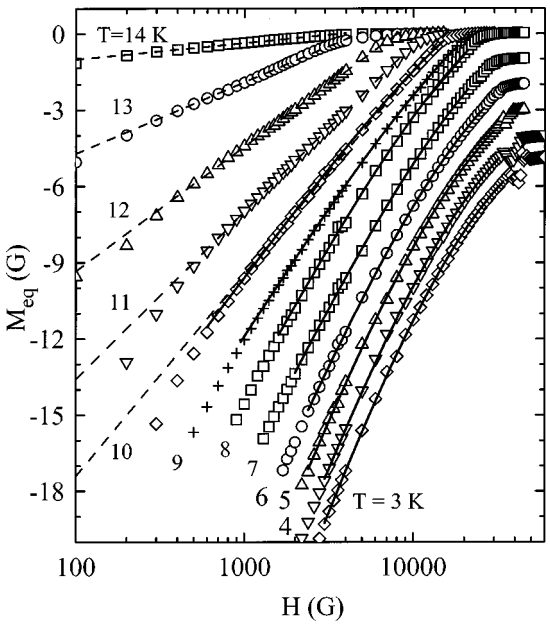

FIG. 2. A semilogarithmic plot of equilibrium magnetization versus H, for temperatures from 14 to 3 K in steps of 1 K. (For $T \leqslant 8$ K, each successive curve is shifted down by 1 G.) Local London theory [Eq. (1)] predicts the linear dependence (dotted lines) seen at higher temperatures, but cannot account for the curvature at lower temperatures. Nonlocal London theory [Eq. (2), solid lines] describes the data well.

from three independent length scales—ρ, λ, and ξ. To verify proper behavior, the temperature dependencies of the parameters are presented in Fig. 3. The nonlocal theory predicts that the field scale H_0, shown in Fig. 3(a), should be constant at low temperature and then increase for temperatures nearer T_c. Experimentally, the field is approximately constant for $t = T/T_c \lesssim \sim 0.4$, after which it rises steadily, qualitatively very similar to the features observed in the original analysis[6] of $Bi_2Sr_2CaCu_2O_x$ and $Tl_2Ba_2CaCu_2O_x$ high-T_c materials. From the relation $H_0 = \phi_0/(4\pi^2\rho^2)$, we obtain the value $\rho = 31$ Å for $T \ll T_c$. A further consistency check comes from evaluating the quantity $\gamma(T)H_0(T)$, where the parameter $\gamma(T)$ gives the temperature dependence of the nonlocality radius ρ. (Values for γ were calculated by Kogan *et al.*, and have been taken from Fig. 1 of Ref. 6, using a ''clean'' scattering parameter $\xi_0/l = 0.3$; here ξ_0 is the BCS coherence length and $l \approx 300$ Å is the electronic mean free path, estimated from the electrical resistivity at 20 K.) According to the nonlocal theory, the product $\gamma(T)H_0(T)$ should be constant; the observed temperature independence of this quantity, shown in Fig. 3(a) provides a major consistency test for the analysis.

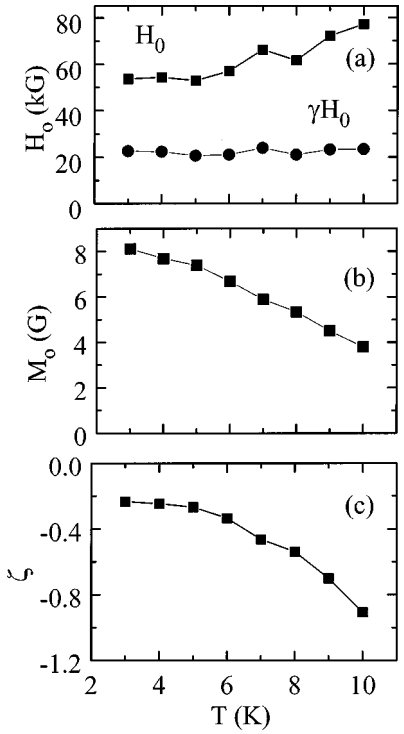

FIG. 3. Parameters from nonlocal London analysis versus temperature: (a) the field scale H_0 (■) and product $\gamma(T)H_0(T)$ (●) (which theoretically should be constant), (b) the magnetization M_0, and (c) dimensionless quantity ζ.

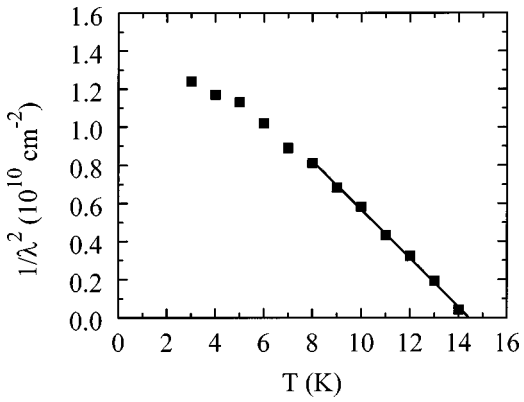

FIG. 4. The London penetration depth λ, obtained with field $H \| (001)$. The straight solid line shows Ginzburg-Landau behavior near T_c.

The temperature dependencies of M_0 and ζ are shown in Fig. 3(b) and 3(c). Both vary smoothly and are qualitatively similar to the results for the high-T_c materials.[6] The London penetration depth extracted from $M_0 \propto 1/\lambda^2$ is shown versus T in Fig. 4. For 10 K and below, the results come from the nonlocal analysis; above 10 K, a conventional London analysis was used. We note that the plot of $1/\lambda^2$ versus T is linear near T_c, as expected from Ginzburg-Landau theory, and it extrapolates to zero near the T_c measured in a low field. Fitting the higher temperature data to a BCS-clean limit temperature dependence yields the value $\lambda(0) = 980$ Å; however, the penetration depth varies faster at low temperatures than predicted by BCS theory. An empirical extrapolation to $T = 0$ yields the value $\lambda(0) = 900$ Å. This value lies about 15% below the previous determinations of Yethiraj *et al.*[3] and Eskildsen *et al.*,[2] which were obtained from analysis of the neutron-diffraction intensity. It is significantly smaller than the value (~1500 Å) deduced by Xu *et al.*[9] from a conventional London analysis.

The magnetization study also provides information on the upper critical field, yielding a slope $dH_{c2}(T)/dT = -3.8$ kG/K near T_c. More interestingly, we find that at $3\text{ K} \approx 0.2 \times T_c$, the superconductive magnetization goes to zero at 45 kG (see Fig. 1 for corresponding data at 5 K). Taking this as the upper critical field $H_{c2}(T) = \phi_0/2\pi\xi^2$

yields a Ginzburg-Landau coherence length $\xi = 86$ Å, which agrees within experimental error with the result of Eskildsen *et al.*[2] from neutron scattering from a ''transforming FLL'' crystal at 2.2 K. The present results and standard relations for the thermodynamic critical field H_c then give a depairing current density $J_0 = cH_c/(6^{1/2}3\pi\lambda_{ab}) \approx 1.5\times 10^8$ A/cm^2 at low temperatures (here c is the speed of light). As noted above, the $J_c \approx 10^{-6}\times J_0$, meaning that the superconductor is relatively clean and electron scattering is weak, as is necessary for observing pronounced effects of nonlocality. Continuing, the measured electrical resistivity and other material parameters[10] provides an estimate for the electronic mean free path, $l \approx 300$ Å. This significantly exceeds the coherence length, again reinforcing the idea that the clean material enables nonlocality effects to be observed. Finally, one can use the Pippard relation $(1/\xi) = (1/\xi_0) + (1/l)$ to estimate the BCS coherence length $\xi_0 \approx 120$ Å at $T = 0$. This is somewhat smaller, but roughly comparable with the values deduced by Metlushko *et al.*[11] for $LuNi_2B_2C$.

In conclusion, the equilibrium magnetization of this clean, reversible YNi_2B_2C crystal qualitatively deviates from what is predicted by traditional local London theory, but accurately follows the form of nonlocal London theory. The resulting parameters behave as the nonlocal theory prescribes, with a well-behaved penetration depth $\lambda(T)$. Thus the nonlocal London theory provides a common basis for understanding both the macroscopic magnetization study and microscopic neutron-scattering experiments.

We wish to acknowledge valuable discussions with V. G. Kogan, P. Miranovic, and L. Krusin-Elbaum. A portion of the work of J.R.T. was supported by the UTK-ORNL Science Alliance. Oak Ridge National Laboratory is managed by Lockheed Martin Energy Research Corp. for the U.S. Department of Energy under Contract No. DE-AC05-96OR22464.

[1] D. McK. Paul, C. V. Tomy, C. M. Aegerter, R. Cubitt, S. H. Lloyd, E. M. Forgan, S. L. Lee, and M. Yethiraj, Phys. Rev. Lett. **80**, 1517 (1998).

[2] M. R. Eskildsen, P. L. Gammel, B. P. Barber, A. P. Ramirez, D. J. Bishop, N. H. Andersen, K. Mortensen, C. A. Bolle, C. M. Lieber, and P. C. Canfield, Phys. Rev. Lett. **79**, 487 (1997).

[3] M. Yethiraj, D. McK. Paul, C. V. Tomy, and E. M. Forgan, Phys. Rev. Lett. **78**, 4849 (1997).

[4] Y. De Wilde, M. Iavarone, U. Welp, V. Metlushko, A. E. Koshelev, I. Aranson, and G. W. Crabtree, Phys. Rev. Lett. **78**, 4273 (1997).

[5] V. G. Kogan, M. Bullock, B. Harmon, P. Miranovic, Lj. Dobrosavljevic-Grujic, P. L. Gammel, and D. J. Bishop, Phys. Rev. B **55**, R8693 (1997).

[6] V. G. Kogan, A. Gurevich, J. H. Cho, D. C. Johnston, Ming Xu, J. R. Thompson, and A. Martynovich, Phys. Rev. B **54**, 12 386 (1996).

[7] I. Affleck, M. Franz, and H. H. Sharifzadeh, Phys. Rev. B **55**, R704 (1997).

[8] V. G. Kogan, M. M. Fang, and Sreeparna Mitra, Phys. Rev. B **38**, 11 958 (1988).

[9] Ming Xu, P. C. Canfield, J. E. Ostensen, D. K. Finnemore, B. K. Cho, Z. R. Wang, and D. C. Johnston, Physica C **227**, 321 (1994).

[10] S. V. Shulga, S.-L. Drechsler, G. Fuchs, K. H. Mueller, K. Winzer, M. Heinecke, and K. Krug, Phys. Rev. Lett. **80**, 1730 (1998).

[11] V. Metlushko, U. Welp, A. Koshelev, I. Aranson, G. W. Crabtree, and P. C. Canfield, Phys. Rev. Lett. **79**, 1738 (1997).